

# DATA FUSION FOR GEOTHERMAL RESERVOIR CHARACTERIZATION

Maria Gudjonsdottir<sup>1</sup>, Cari Covell<sup>1</sup>, Léa Lévy<sup>2,4,5</sup>, Agust Valfells<sup>1</sup>, Juliet Newson<sup>1</sup>, Egill Juliusson<sup>3</sup>, Halldor Pálsson<sup>2</sup>, Birgir Hrafnkelsson<sup>2</sup>, Samuel Scott<sup>1</sup>

<sup>1</sup>Reykjavik University, Menntavegur 1, 102 Reykjavik, Iceland

<sup>2</sup>University of Iceland, Saemundargata 2, 101 Reykjavik, Iceland

<sup>3</sup>Landsvirkjun, National Power Company of Iceland, Haaleitisbraut 68, 103 Reykjavik, Iceland

<sup>4</sup>Ecole Normale Supérieure, Paris, France

<sup>5</sup>ÍSOR, Iceland GeoSurvey, Grensásvegur 9, 108 Reykjavik, Iceland

msg@ru.is

**Keywords:** *Geologic modeling, Rock properties, Gravity data, Bayesian inference, Krafla Iceland.*

## ABSTRACT

This study performs Bayesian inversion of geophysical (gravity) data to generate probabilistic 3D subsurface models. Probabilistic models describe the uncertainty of model predictions, which is beneficial for managing risk during decision making such as well position targeting. We select Krafla geothermal system in Iceland as a case study for the application of three-part framework. The method combines a prior geologic model of the area based on primary geologic data obtained from wells, statistical analysis of petrophysical properties (density and porosity) based on available databases and additional measurements, as well as available gravimetric measurements data. A Markov chain Monte Carlo sampling scheme, implemented in the geological modelling software GeoModeller, is used to invert for subsurface lithology and density. Due to the non-uniqueness of gravity data, many possible models of subsurface density distribution could account for the measured data. The a priori uncertainty of the lithological model largely controls the uncertainty of the posterior results for lithology and density. This shows that reliable prior geological constraints are important in Bayesian inversion. In this case, the lithological model consists of layers of high-density lava flows and low-density hyaloclastites underlain by high-density basement intrusions. Rock density depends also significantly on the extent and type of hydrothermal alteration particularly for hyaloclastites where density tends to be higher with increased extent of alteration. More realistic prior density probability density functions (pdf's) especially accounting for hydrothermal alteration for hyaloclastites result in more realistic model output.

## 1. INTRODUCTION

Geothermal scientists model reservoirs using a wide variety of data acquired from various sources. While many different models of the reservoir can be made that address some subset of the available data, the challenge that this project addresses is to create models that can best fit many types of available data. This research project, Data Fusion for Geothermal Reservoir Characterization, started in 2017 and is intended to combine data from geophysical, geological, and hydrological surveys through a data fusion and joint inversion process to create more realistic reservoir models. The overall goal is to assess geothermal development risks and create more realistic reservoir models that can assist in decision making for geothermal development.

The method described here, combines statistical analysis of rock properties, with a prior geological model presenting an interpretation of the litho-stratigraphy of the area based on drill cuttings. The aim is to reduce the uncertainty of this prior model by using observed data such as gravimetric measurements. Prior geologic models can be linked to observed geophysical data by petrophysical data, which can be used to parameterize the prior probability distribution functions (pdfs) for the bulk density of the lithological units in the prior model. A Markov Chain Monte Carlo sampling scheme is used to obtain millions of realizations of posterior lithologic and density structures consistent with the measured data (Bosch, 1999; Bosch et al., 2001). Since gravimetric data describe variations of subsurface density, statistics for grain density and porosity are needed to parameterize prior pdf's of different lithological units. Similar probabilistic inversions for resistivity structures could be carried out, using magneto-telluric (MT) data and methods to integrate resistivity to temperature and permeability have been performed on synthetic MT data (Dempsey et al., 2019; Ardid et al., 2019). There is however comparatively limited available petrophysical data to parameterize pdf's for resistivity data and in addition, resistivity is also dependent on temperature and fluid composition (Levy et al., 2018).

Rock properties such as grain density, total porosity, and permeability also control the mechanical behavior of rocks and productivity of aquifers. Therefore, by helping to constrain the spatial heterogeneity of rock type and physical property distributions, these probabilistic geologic models reduce uncertainty in reservoir modeling. In this study, we examine variability in grain density, total porosity, and permeability between the main lithologies and alteration zones found in Icelandic geothermal systems, with the aim of finding the best way to represent the data using statistical distributions for each litho-type. Hydrothermal alteration affects the density and porosity of Icelandic rocks, particularly hyaloclastites (Franzson et al., 2011). In addition to the physical property distributions for each lithology, the uncertainty of the prior reference geologic model also strongly influences inversion results. In this study, we constrain the lithologic structure of model realizations by assuming some overlap between the prior reference model and model realizations, and observe how the degree of overlap controls the inversion results.

We select the Krafla geothermal system in northeast Iceland as a case study for the application of the Bayesian inference methodology due to the availability of a well-constrained geologic model (Mortensen et al., 2009; Weisenberger et al., 2015) as well as recent gravimetric data (Magnússon, 2016).

## 2. METHODS

### 2.1 Krafla geothermal system

Krafla is one of five active volcanic centers arranged in enechelon fashion within the northern volcanic zone (NVZ) in northeast Iceland. The Krafla area features a volcanic caldera astride a major NNE-SSW trending fissure swarm (Saemundsson, 2008). In this project we use results from gravity surveys and available reference geologic model for the system. The gravity data used in this study is described in detail by Magnusson (2016), which considers 522 measurements made over an area of ~625 km<sup>2</sup>. Following Magnusson (2016), the residual Bouguer anomaly is calculated assuming a reference density of 2.51 g cm<sup>-3</sup>. Figure 1 illustrates the structure of the Krafla caldera; topography, density variations (represented by Bouguer anomalies), fissure swarms and caldera rims.

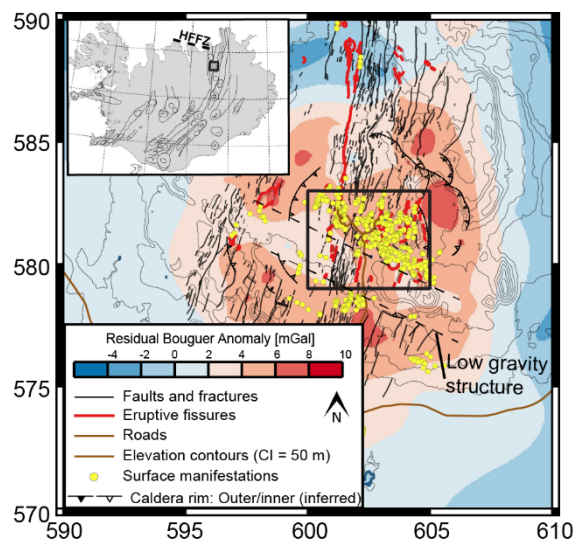


**Figure 1: Topographic map of the Krafla area showing Residual Bouguer anomaly, geothermal surface manifestations, eruptive fissures and craters, outer caldera rim, inferred inner caldera rim and roads. Dashed lines show boundary of low gravity structure. Box shows the area of the geologic model built in this study. Coordinates are shown in ISNET95 (same as Lambert 95).**

The reference geologic model of the Krafla system is developed based on surface geologic mapping (Saemundsson, 2008) and an interpreted 3D geologic model for the system previously built in Petrel (Mortensen et al., 2009; Weisenberger et al., 2015). Figure 2 shows the surface geology within the model domain (the area of which is shown inside the box in Figure 1) as well as the location of cross-sections shown in Figures 2b-d. The reference geologic model presents a simplified interpretation of the complex sequence of lithologic units identified from well cuttings (Mortensen et al., 2009 and references therein). The eleven stratigraphic units consist of an alternating sequence of lava flow units (L1-L5, shown in blue-green) and hyaloclastite units (H1-H4, yellow) underlain by basement intrusions (B, red) and overlain in some areas by a thin (<0.2 km) surface cover (grey). The geologic model in Figure 2 is based on wellbore data (cuttings) from a small area within the area of 25 km<sup>2</sup> which the geologic model represents.

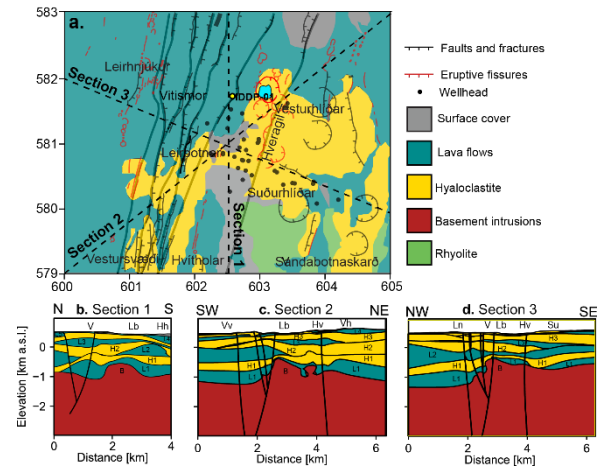


**Figure 2: Reference geologic model of the Krafla system.**

**a. Surface geologic map of Krafla caldera, showing mapped faults and fractures (grey), eruptive fissures (red), and locations of wells (black dots), as well as the surface traces of Section 1-3. (b-d) Fault structure is calculated based on the assumption of near vertical dips and is highly uncertain. Rhyolites are not included in the geologic model but shown in the surface geologic map. Coordinates in the surface map are shown in ISNET95 (same as Lambert 95).**

### 2.2 Rock property data

Many studies have investigated the physical and chemical properties of Icelandic geothermal reservoir rocks (e.g. Sigurdsson et al., 2000; Franzson et al., 2001; Frolova et al., 2005; Franzson et al., 2011). This study is part of an ongoing effort to merge all of the available rock property data from samples collected throughout Iceland into the Valgarður database. Presently, the database mainly consists of surface samples collected between the years 1992-2004 (786 samples) and drill cores from Krafla (16 samples). Measured data include a description of geology and mineralogy, chemical analyses and petrophysical properties (grain density, total porosity, and gas permeability corrected for the Klinkenberg effect). However, not all types of measurements are available for all samples.

In addition to Valgarður database, a complementary dataset obtained on core samples from four boreholes at Krafla volcano (boreholes KH1, KH3, KH5 and KH6) that was published by Lévy et al. (2018) was used here. Additional 32 samples were recently collected and analyzed (mineralogy characterization and petrophysical measurements) in the frame of this project. 16 of these new samples come from Krafla (borehole KH3) and 16 others from borehole THR-7 in Theistareykir. These two datasets include density and porosity measurements, as well as XRD mineralogical quantification.

Finally, data from various geothermal sites around the world, gathered into a database compiled by Bär et al. (2017) within the Integrated Methods for Advanced Geothermal Exploration (IMAGE) project, is used for comparison of petrophysical data, but only the Icelandic samples are used in this analysis.

## 2.3 Bayesian inference framework

To create a posterior lithologic structure of the area from the prior geologic model (shown in Figure 2) and observed gravity data (shown in Figure 1), a Bayesian inference framework implemented in the GeoModeller software package (Intrepid Geophysics, 2017a, 2017b) was used to perform these calculations. GeoModeller uses a Markov Chain Monte Carlo (MCMC) statistical sampling scheme to drive the litho-constrained 3D inversion process and to evaluate the posterior probability distribution and density distribution. A detailed description of the method can be found in literature (Bosch, 1999; Bosch et al., 2001; Guillen et al., 2008). Measurements of the gravity potential field are used to estimate the posterior probability density functions for lithology and density throughout the model domain according to a modified version of Bayes' law shown in Equation (1).

$$\pi(m_{\text{sec}}, m_{\text{pri}} | y) = c L(y | m_{\text{sec}}) \pi_{\text{sp}}(m_{\text{sec}} | m_{\text{pri}}) \pi_p(m_{\text{pri}}) \quad (1)$$

The Bayesian inference scheme divides the prior probability space into a primary geologic parameter space ( $m_{\text{pri}}$ ) describing the spatial distribution of the lithologies and a secondary parameter space ( $m_{\text{sec}}$ ) describing rock petrophysical properties conditional on lithology. The posterior pdf  $\pi(m_{\text{sec}}, m_{\text{pri}} | y)$  represents the updated knowledge about the subsurface lithologic and density distribution given the observed gravity data  $y$ . This quantity is proportional (up to a normalization constant  $c$ ) to the product of the two prior pdfs, one considering the primary lithological subspace  $\pi_p(m_{\text{pri}})$  and a conditional pdf describing the dependence of the bulk (wet) density on the lithology  $\pi_{\text{slp}}(m_{\text{sec}} | m_{\text{pri}})$ , and a likelihood function  $L(y | m_{\text{sec}})$ , which quantifies probabilistically the misfit between the gravity potential field calculated from the joint model and the observed gravity data.

## 3. RESULTS AND DISCUSSION

### 3.1 Probability distributions of rock properties

Figure 3 shows three plots including petrophysical properties and lithological classification of all data mentioned in Section 2.2. By visual inspection, Figure 3a shows the hyaloclastites with the majority of porosity measurements  $> 10\%$  and at grain densities  $< 2.8 \text{ g/cm}^3$ . Many of the unknown samples are on trend with intrusion measurements, i.e. high grain density and low porosity, but several are hard to distinguish, especially between hyaloclastite and lava flow. In Figure 3b, there is fairly clear separation of hyaloclastite and lava, where hyaloclastite have high porosity and high permeability (majority  $> 10^1 \text{ mDa}$ ) compared to lava having lower porosity and lower permeability. However, several intrusion measurements also follow lava pattern, making it difficult to identify differences in these rock property measurements based on those lithologies. Finally in Figure 3c, hyaloclastite follow the trend of low grain density and high permeability. Once again, many lava and intrusion measurements seem to be mixed but together follow the trend of higher grain density and lower permeability than hyaloclastite. This could be due to the phenomenon of a lava flow having a dense core, with vesicles of high porosity in the upper and lower part. Therefore, some samples within lavaflows and intrusives are misclassified, or a different category of lithology exists that should be more detailed when describing samples in a database. The unknown samples are also quite mixed and

scatter throughout the dataset, therefore showing potential for lithological characterization once more analyses have been done to clearly distinguish the known lithologies.

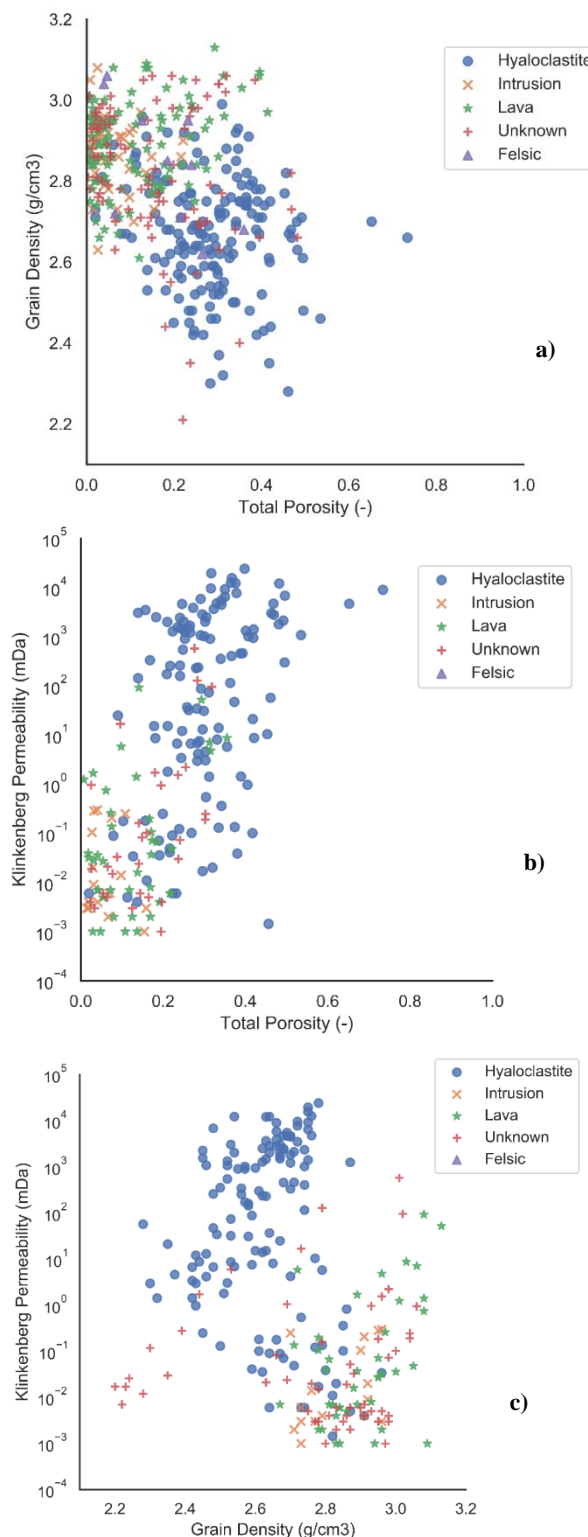


**Figure 3: Scatter plots of petrophysical properties categorized by lithology. a) Total porosity versus grain density. b) Total porosity versus Klinkenberg permeability. c) Grain density versus Klinkenberg permeability.**

Figure 4 shows the distribution of rock bulk density distribution for the three lithologic units which our prior model consisted of (lava flows, hyaloclastite and basement intrusions) as well as the mean ( $\mu$ ) and standard deviation ( $\sigma$ ) of the distribution. The prior probability density functions (pdfs) for the bulk density of each rock type were calculated by fitting a normal distribution to 10,000 samples obtained through the Monte Carlo sampling. We calculate a posterior but show model results in terms of most probable lithology. Note that the data used for the distribution calculations are from the earlier Valgarður database only.

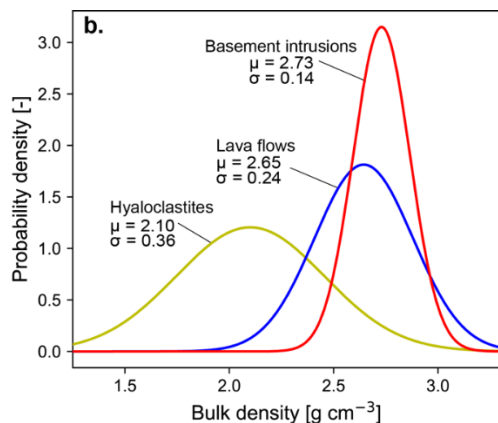


**Figure 4. Prior probability distribution functions (pdfs) for bulk (wet) density obtained through Monte Carlo sampling used as input for the calculations in GeoModeller.**

### 3.2 Comparison of Density Values

Figure 5 shows the three stages of the observed or calculated gravity data for the geologic model of the Krafla field. Figure 5a shows the observed data from gravity measurements (Residual Bouguer Anomaly). Figure 5b shows the density of the reference prior geologic model, based on the lithology and assuming mean bulk density values for each type of lithology (lava flow, hyaloclastites or basement intrusions) and Figure 5c shows the calculated gravity values after the inversion process.

The inversion process reduces misfit between the forward modeled gravity potential field and the measured data. Initially, the gravity field calculated using the reference prior model assuming mean properties for each rock type (Fig. 5b) predicts higher gravity values (6-12 mGal) than the observed data (Fig. 5a, 2-6 mGal). While the mean bulk density-only reference prior model predicts lower gravity values in the SW between Leirbotnar and Vestursvæði, similar to the observed data set, a low gravity anomaly in the NW of high gravity anomalies in the SE are not seen in the observed data, which predicts low gravity in the SE. After the inversion process, there is a close correspondence between the gravity field calculated for the changed model and the measured data, with the absolute misfit less than 0.3 mGal (Fig. 5c). Note that Fig. 5c shows results at the end of an inversion run; the gravity field calculated varies slightly depending on the step in the inversion process and the run configuration. However, the absolute misfit values during the inversion process are nearly constant (0.1 mGal RMS), close to the uncertainty of the data, and generally similar between different model runs.

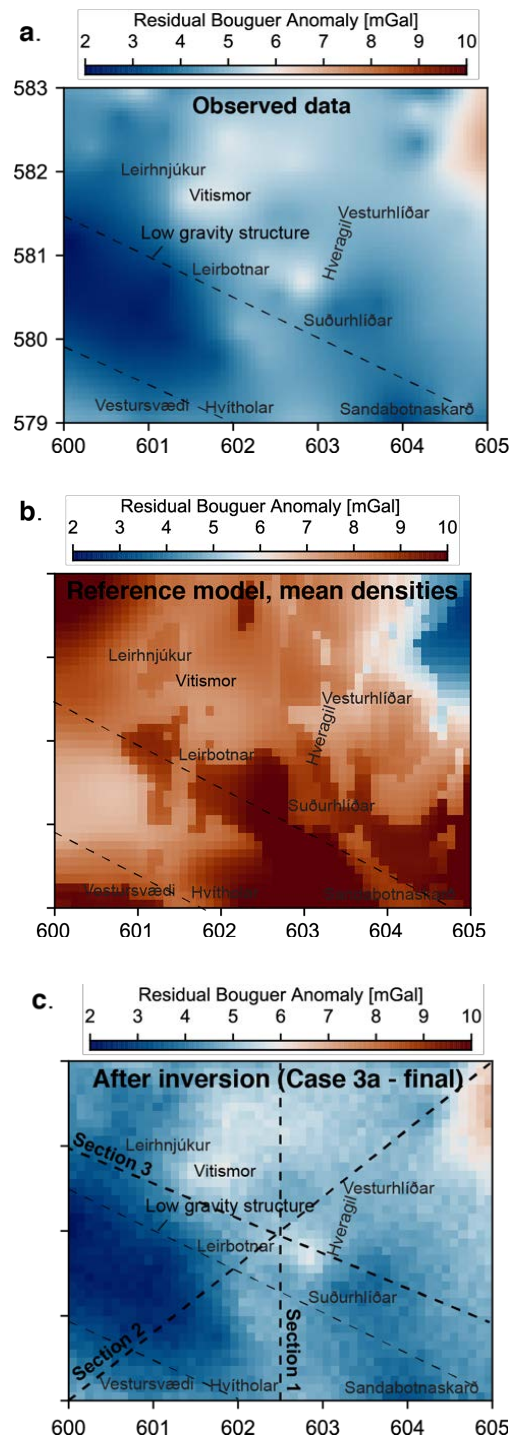


**Figure 5. Comparison between observed and modeled gravity data. a. Observed Residual Bouguer anomaly in the model area b. Calculated residual Bouguer anomaly with reference prior geologic model assuming mean bulk densities for each type of lithology. c. Calculated residual Bouguer anomaly after inversion process.**

Figure 6 shows the comparison of the prior geologic model (Figure 6a, same as Figure 2b) and the most likely posterior model after the inversion process (Figure 6b). The outline of

the borders of the lithologic units from Figure 6a are kept the same in Figure 6b.

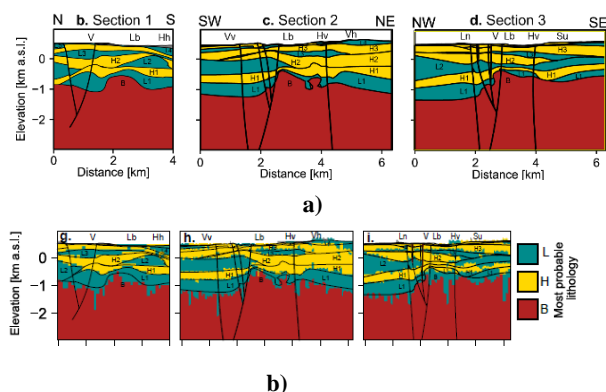


**Figure 6: Comparison of the prior geologic model used for the Krafla area (a) and the most probable model after the inversion process (b).**

The uncertainty of model predictions depends on the strength of the geologic constraints imposed on the probabilistic inversions (Scott et al., in press). In this study, the commonality metric is used to probabilistically constrain the expected overlap between the lithologic structure of the prior reference model and the model realizations and invert for voxel lithology and bulk density. Other approaches invert directly for contact point and orientation measurements (e.g. Wellman et al., 2017; De La Varga et al., 2019). However, in our case the reference prior geologic model used in this study represents only an interpretation of the stratigraphic data, we take a different approach. A commonality constraint quantifies the overlap in voxel lithology between a model realization and the prior reference geologic model. A moderate strength commonality constraint preserves the resemblance to the geologic prior model in the results for posterior lithologic structure, while also allowing divergence between the prior and posterior in areas where the prior model may be inconsistent with the gravity data and may thus need to be altered. Figure 7 compares the most probable lithologic models for the three inversion runs using a moderate commonality constraint: 1) a base-case scenario (similar to Figure 6); 2) the same reference prior geologic model but with the bulk density of the hyaloclastite units increased to account for the effects of alteration; and 3) a prior reference geologic model that includes a rhyolitic intrusion in the vicinity of Vitismor (consistent with the evidence from the Iceland Deep Drilling Project IDDP-01 well, which encountered a shallow intrusion in the vicinity beneath this area).

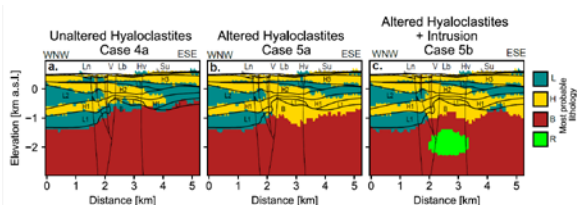


**Figure 7. Comparison of posterior results for different inversion runs. See text for description of different inversion runs.**

### 3.3 Petrophysical properties based on alteration

Similar to the scatter plots based on lithology in Figure 3, three different comparisons were made between grain density, total porosity, and Klinkenberg permeability, based on alteration zone and using data from the Valgardur database are shown in Figure 8a-c.

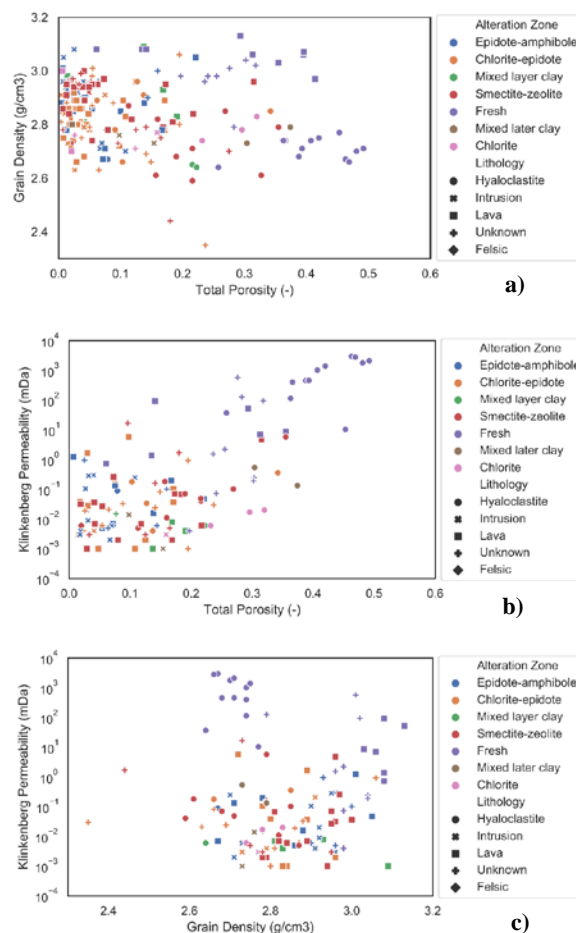


**Figure 8: Scatter plots of petrophysical properties categorized by alteration zone (colour) for the lithologies (symbol). a) Total porosity versus grain density. b) Total porosity versus Klinkenberg permeability. c) Grain density versus Klinkenberg permeability.**

Figure 8 suggests that fresh (unaltered) samples have higher porosity (>20%) and higher permeability (>1 mDa). Grain density and total porosity depend on the alteration zone, with samples altered to smectite-zeolite or mixed-layer clay facies having lower density and higher porosity than samples altered to chlorite-epidote or epidote-amphibole facies. However, there are also a cluster of samples with smectite-zeolite alteration that show low porosity (<10%). Klinkenberg permeability ranges over six orders of magnitude and increases with porosity. The mixed layer clays also have good clustering for total porosity (<20%) when compared to both grain density and Klinkenberg permeability, however not as much agreement when comparing grain density and Klinkenberg permeability side by side. Here, these differences show variability in best comparisons of petrophysical measurements to alteration zones.

Comparison between porosity and alteration quantity are shown in Figure 9 for data by Lévy et al. (2018) along with the 32 new samples measured by one of the authors (Covell).

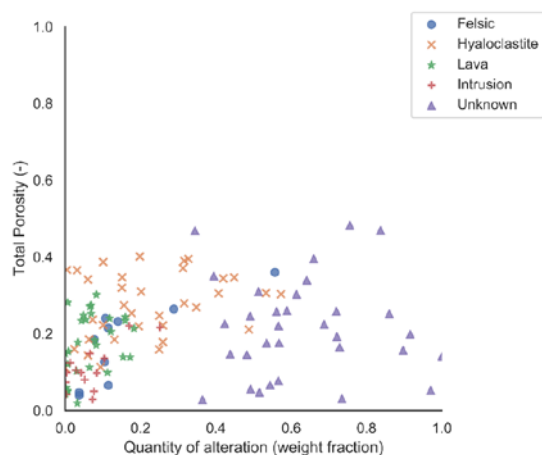


**Figure 9: Scatter plot of altered crystals (weight fraction) with respect to total porosity, categorized by lithology in Levy and Covell data**

From Figure 9 it can be seen that interestingly, intrusions are not highly altered from these samples. The unknown category has high alteration separate from all the other categories, so this may be a separate class or two classes of lithology perhaps one of highly altered hyaloclastites and one of highly altered intrusions, based on the porosity. As this cluster is visually closer to the hyaloclastite cluster (compared to the lava cluster), perhaps many of these samples are behaviorally like highly altered hyaloclastites.

#### 4. CONCLUSION

In this study we have combined a reference prior geologic model built from borehole data, statistical analysis of rock properties and gravimetric data in a Bayesian inference framework to generate a probability distribution for the distribution of major lithologies and subsurface density distribution. A companion study shows the uncertainty of the prior affects posterior probabilities and uncertainty quantification metrics obtained by probabilistic, litho-constrained inversion of gravity data (Scott et al., in press). Bayesian inversion methods allows knowledge of the structure and properties of the subsurface to constrain the inversion. However, while rock petrophysical properties are measured in the lab and may be known with some confidence, there is uncertainty stemming from changes in rock properties of rock samples between the surface and depth. However, the greater uncertainty may lie with the geologic structure.

The main lithologies present in each of the databases overall are hyaloclastite, lava, and intrusion. However, many lithologies are unknown, but are likely to be either hyaloclastite or lava flow. In terms of mineralogy, smectite-zeolites and mixed layer clays have some trend of agreement, in terms of porosity compared with either grain density or Klinkenberg permeability, within the Valgardur and IMAGE database collaboration. Within altered crystals, trends for hyaloclastites show enough variability where the category may need to be split into two or more groups. For overall alteration within the Levy and Covell data, many of the

unknown samples could belong to their own category, or perhaps be a portion of highly altered hyaloclastites.

As this is a work in progress, further studies will detail K nearest neighbors analyses for the unknown category, and potentially the basaltic/pillow breccia category. The methodology described here will be used further where Bayesian inversion is performed of natural state temperature and pressure data to generate probabilistic 3D subsurface models.

#### ACKNOWLEDGEMENTS

The work presented here was funded by RANNIS, The Icelandic Centre for Research under the Technology Development Fund and Landsvirkjun Energy Research Fund. The Valgardur Database was used with permission from Landsvirkjun. Access to the IMAGE database was with permission from Kristian Bär of Technische Universität Darmstadt. We would also like to thank Hjalti Franzon from ISOR for providing assistance with Valgardur data analysis. We also thank Benoit Gibert, David Escobedo and Bernard Fraisse from University of Montpellier for their support and help with petrophysical and XRD measurements.

#### REFERENCES

- Ardid, A., Dempsey, D., Bertrand, T. and Archer, R. Uncertain Estimation of Subsurface Temperature Away from the Borehole Using Magnetotelluric Inversions. In *Proceedings 40<sup>th</sup> New Zealand Geothermal Workshop*. (2018).
- Bar, K., Reinsch, T., Sippel, J., Strom, A., Mielke, P., and Sass, I. P<sup>3</sup>-International PetroPhysical Property Database. In *Proceedings, 42nd Workshop on Geothermal Reservoir Engineering, Stanford University, Stanford, CA* (pp. 1-6). (2017).
- Bosch, M.: Lithologic Tomography: From Plural Geophysical Data to Lithology Estimation. *J. Geophys. Res. Solid Earth* **104**, (1999), 749–766.
- Bosch, M., Guillen, A. and Ledru, P.: Lithologic Tomography: An Application to Geophysical Data from the Cadomian Belt of Northern Brittany, France. *Tectonophysics* **331**, (2001), 197–227.
- De la Varga, M., Schaaf, A. and Wellmann, F.: GemPy 1.0: Open-Source Stochastic Geological Modeling and Inversion. *Geosci. Model Dev.* **12**, (2019).
- Dempsey, D., Riffault, J., Ardid, A., Bertrand, T. and Archer, R. Toward Magnetotelluric and Microseismic Calibration of Geothermal Reservoir Models. In *Proceedings 44<sup>th</sup> Workshop on Geothermal Reservoir Engineering, Stanford University*. (2019)
- Franzson H., Gudlaugsson, S., and Fridleifsson, G.O.: Petrophysical properties of Icelandic rocks. *Proceedings, Sixth Nordic Symposium on Petrophysics, Trondheim, Norway*. (2001)
- Franzson, H., Gudfinnsson, G.H., Frolova, J., Helgadóttir, H., Mortensen, A.K. and Jakobsson S.P. *Icelandic Hyaloclastite Tuffs*. Tech. Rep., ISOR-2011/064, (2011)
- Frolova, J.V., Ladygin, V.M., Franzson, H., Sigurðsson, O., Stefánsson, V. and Shustrov, V.: Petrophysical Properties of Fresh to Mildly Altered Hyaloclastite

- Tuffs. *Proceedings, World Geothermal Congress, Antalya, Turkey*, (2005).
- Guillen, A., Calcagno, P., Courrioux, G., Joly, A., and Ledru, P. Geological Modelling from Field Data and Geological Knowledge: Part II. Modelling Validation Using Gravity and Magnetic Data Inversion. *Physics of the Earth and Planetary Interiors*, **171**, (2008), 158–169.
- Intrepid Geophysics: *3D GeoModeller Reference*, (2017a)
- Intrepid Geophysics: *Forward Modeling and Inversion with 3D GeoModeller*, (2017b)
- Levy, L., Gibert, B., Sigmundsson, F., Flovenz, O. G., Hersir, G. P., Briole, P., & Pezard, P. A. (2018). The role of smectites in the electrical conductivity of active hydrothermal systems: electrical properties of core samples from Krafla volcano, Iceland. *Geophysical Journal International*, 215(3), 1558-1582.
- Magnússon, I.P.: Gravity Measurements at Theistareykir in July-September 2015 and Gravity Map of the Krafla Area. Tech. Rep. (Report in Icelandic), *Iceland GeoSurvey*, (2016), LV-2016-090.
- Mortensen, A.K., Gudmundsson, Á., Steingrímsson, B., Sigmundsson, F., Axelsson, G., Ármannsson, H. et al. The Krafla Geothermal Field. Overview of Geothermal Research and a Revised Conceptual Model. (Report in Icelandic). *Iceland GeoSurvey. ÍSOR-2009/057*. (2009).
- Scott, S., Covell, c., Juliusson, E., Valfells, A., Newson, J., Hrafnkelsson, B., Palsson, H., Gudjonsdottir, M.: A Probabilistic Geologic Model of the Krafla Geothermal System Constrained by Gravimetric Data. *Geothermal Energy: Science, Society, and Technology*. (in press).
- Sigurdsson, Ó., Gudmundsson, Á., Fridleifsson, G. Ó., Franzson, H., Gudlaugsson, S. Th., and Stefánsson, V.: Database on Igneous Rock Properties in Icelandic Geothermal Systems. Status and Unexpected Results. *Proceedings, World Geothermal Congress*, (2000)
- Sæmundsson, K. *Krafla geothermal map, 1:25000*. Reykjavík: Landsvirkjun and ÍSOR. (2008).
- Weisenberger, T.B., Axelsson, G., Arnaldsson, A., Blischke, A., Óskarsson, F., Ármannsson, H., Blanck, H., Helgadóttir, H.M., Berthet, J-C., Árnason K., Ágústsson, K., Gylfadóttir, S., and Guðmundsdóttir, V.: Revision of the Conceptual Model of the Krafla Geothermal System. *Iceland GeoSurvey, ÍSOR-2015/012; LV-2015-040* (2015).
- Wellmann, J. F., de la Varga, M., Murdie, R. E., Gessner, K., and Jessell, M. “Uncertainty estimation for a geological model of the Sandstone greenstone belt, Western Australia—insights from integrated geological and geophysical inversion in a Bayesian inference framework.” *Geological Society, London, Special Publications*, 453, (2017), SP453-12.